Electronic Supplementary Information (ESI) for

Chiral Heterobimetallic Chains from a Dicyanideferrite Building Block Including a π- conjugated TTF Annulated Ligand

Long Cui,[†] Zhong-peng Lv,[†] Chanel F. Leong,[‡] Jing Ru,[†] Deanna M. D'Alessandro,[‡] You Song,[†] and Jing-Lin Zuo[*†]

[†]State Key Laboratory of Coordination Chemistry, School of Chemistry and Chemical Engineering, Collaborative Innovation Center of Advanced Microstructures, Nanjing University, Nanjing 210093, P. R. China

[‡]School of Chemistry, The University of Sydney, New South Wales 2006, Australia

[*] To whom correspondence should be addressed. Email: zuojl@nju.edu.cn; Fax: +86-25-83314502. Nanjing University.

Caption of Content

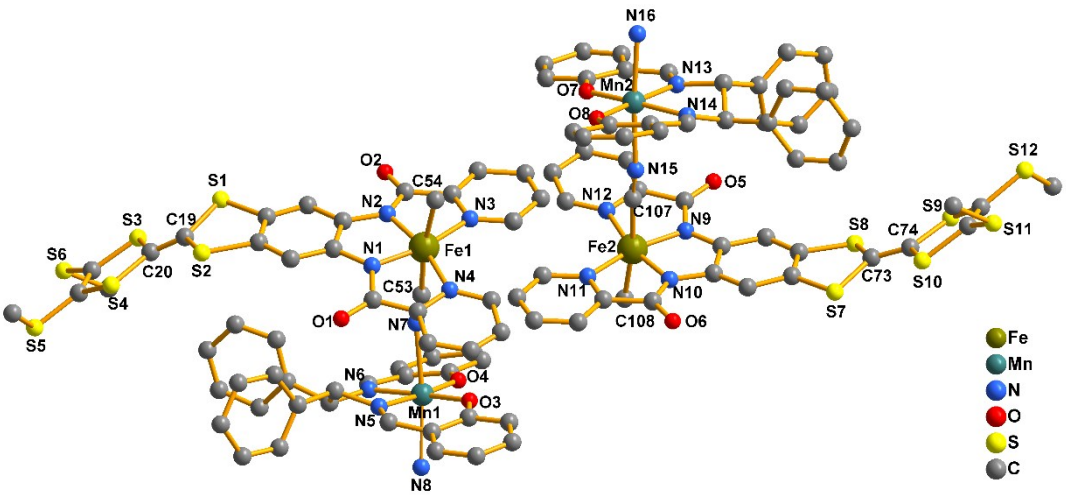

Figure S1. Perspective drawing of the crystallographic structural unit of **2**-(*RR*) showing the atom numbering. Hydrogen atoms are omitted for clarity.

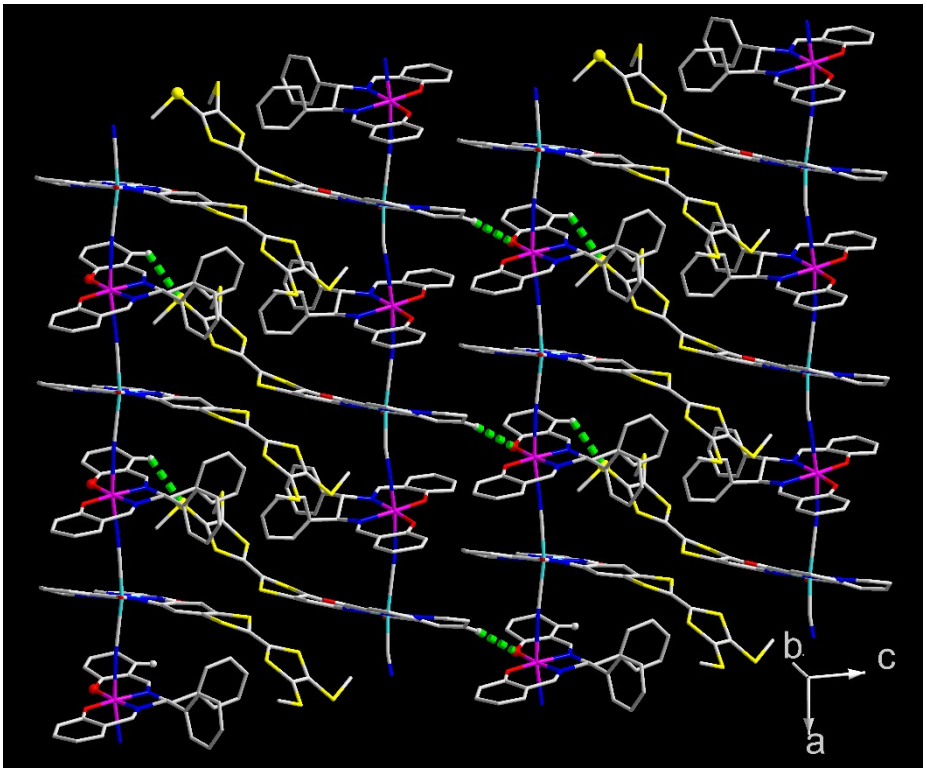

Figure S2. A view showing 2D layer formed by C–H···O and C–H···S interactions (green dash lines) in **2**-(*SS*)

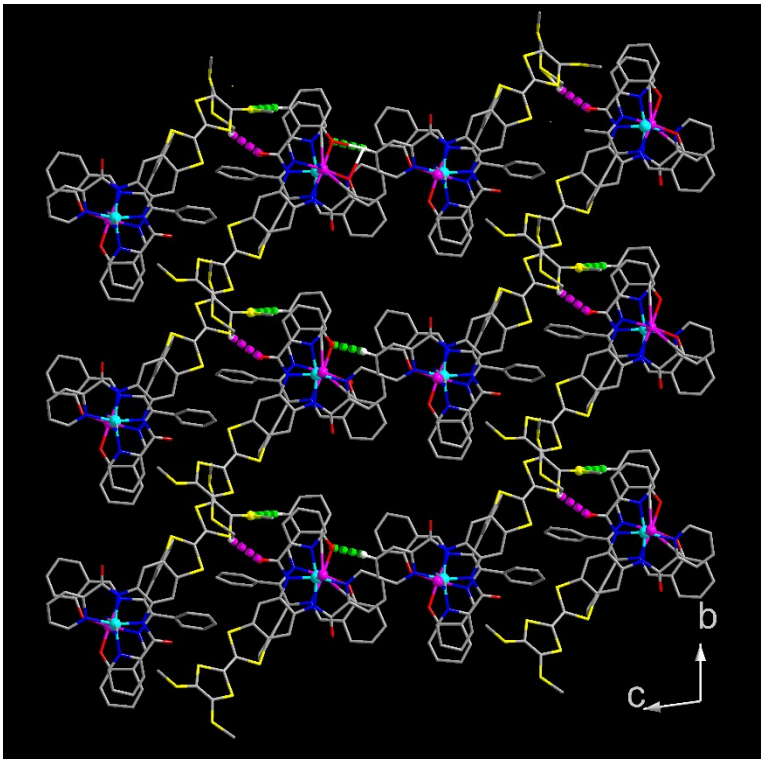

Figure S3. A view showing the 3D structure formed by weak H-bonding interactions (green and pink dashed lines) in **2**-(*SS*).

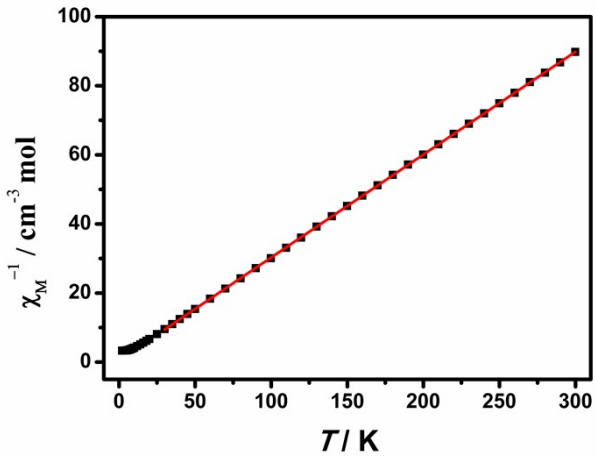

Figure S4. Plot of $1/\chi_M$ vs *T* for **2**-(*SS*). The red solid line is the fitting result from the Curie-Weiss Law.

Table S1. Selected bond lengths (Å) and angles (°) for complex **2-**(*RR*)

Bond Distances (Å)			
Fe(1)-N(1)	1.860(10)	Fe(1)-N(2)	1.899(11)
Fe(1)-N(3)	2.004(11)	Fe(1)-N(4)	1.997(11)
Fe(1)-C(53)	1.964(12)	Fe(1)-C(54)	1.975(13)
Fe(2)-N(9)	1.915(10)	Fe(2)-N(10)	1.867(11)
Fe(2)-N(11)	1.978(12)	Fe(2)-N(12)	1.971(12)
Fe(2)-C(107)	1.963(12)	Fe(2)-C(108)	1.959(12)
C(19)-C(20)	1.317(18)	C(73)-C(74)	1.342(17)
Mn(1)-O(3)	1.883(8)	Mn(1)-O(4)	1.866(8)
Mn(1)-N(5)	1.978(10)	Mn(1)-N(6)	1.999(9)
Mn(1)-N(7)	2.307(9)	Mn(1)-N(8) #1	2.293(10)
Mn(2)-O(7)	1.901(8)	Mn(2)-O(8)	1.880(8)
Mn(2)-N(13)	1.989(10)	Mn(2)-N(14)	1.969(10)
Mn(2)-N(15)	2.255(9)	Mn(2)-N(16) #2	2.216(10)
Bond Angles (°)			
N(7)-C(53)-Fe(1)	174.2(11)	N(8)-C(54)-Fe(1)	175.9(12)
N(15)-C(107)-Fe(2)	176.1(11)	N(16)-C(108)-Fe(2)	172.3(13)
N(1)-Fe(1)-C(53)	90.8(5)	N(2)-Fe(1)-C(53)	89.0(5)
N(1)-Fe(1)-C(54)	96.0(5)	N(2)-Fe(1)-C(54)	95.4(5)
C(53)-Fe(1)-C(54)	172.2(6)	C(53)-Fe(1)-N(4)	87.7(5)
C(54)-Fe(1)-N(4)	89.4(5)	C(53)-Fe(1)-N(3)	88.6(4)
C(54)-Fe(1)-N(3)	85.7(5)	N(10)-Fe(2)-C(108)	93.8(5)
N(9)-Fe(2)-C(108)	93.3(5)	N(10)-Fe(2)-C(107)	90.5(5)
N(9)-Fe(2)-C(107)	92.2(5)	C(108)-Fe(2)-C(107)	173.4(5)
C(53)-N(7)-Mn(1)	153.0(10)	C(54)-N(8)-Mn(1)#2	153.8(10)
C(107)-N(15)-Mn(2)	163.2(11)	C(108)-N(16)-Mn(2)#1	166.8(11)
O(4)-Mn(1)-N(8)#1	93.2(4)	O(3)-Mn(1)-N(8)#1	93.2(4)
N(5)-Mn(1)-N(8)#1	88.3(4)	N(6)-Mn(1)-N(8)#1	86.1(4)
O(4)-Mn(1)-N(7)	93.5(4)	O(3)-Mn(1)-N(7)	88.2(4)
N(5)-Mn(1)-N(7)	84.9(4)	N(6)-Mn(1)-N(7)	91.9(4)
N(8)#1-Mn(1)-N(7)	173.1(4)	O(8)-Mn(2)-N(16)#2	92.0(4)
O(7)-Mn(2)-N(16)#2	94.8(4)	N(14)-Mn(2)-N(16)#2	89.3(4)
N(13)-Mn(2)-N(16)#2	86.9(4)	O(8)-Mn(2)-N(15)	92.8(4)
O(7)-Mn(2)-N(15)	86.7(4)	N(14)-Mn(2)-N(15)	88.7(4)
N(13)-Mn(2)-N(15)	88.2(4)	N(16)#2-Mn(2)-N(15)	174.9(4)

Symmetry transformations used to generate equivalent atoms are given in footnotes #1 to #2.

#1x+1, y, z. #2x−1, y, z.

Table S2. Summary of redox potentials ($E_{1/2}$) of H_2TTFbp, [(n-Bu)$_4$N][Fe(TTFbp)(CN)$_2$] and **2**-(*SS*)

Redox Couple	Redox Potentials (V) *vs.* Fc/Fc$^+$		
	H_2TTFbp	[(n-Bu)$_4$N][Fe(TTFbp)(CN)$_2$]	**2**-(*SS*)
TTF/TTF$^{\bullet+}$	0.15	−0.06	0.37*
TTF$^{\bullet+}$/TTF^{2+}	0.31	0.41	0.89*
Red1	−2.26*	-	-
Red2	−2.43	-	-
Red3	−2.54	-	-
Fe$^{3+/4+}$	-	0.78	-
Fe$^{3+/2+}$	-	−1.16	−0.66*
Mn$^{3+/4+}$	-	-	1.10*

*Reported are E_{ondset} potentials of irreversible processes